Robust Spectral-Domain EM Modeling of Distributed-Source Sensors in Planar-Layered Media

Kamalesh Sainath and Fernando L. Teixeira
ElectroScience Laboratory, Department of Electrical and Computer Engineering
The Ohio State University, Columbus, Ohio 43212 USA
Email: {sainath.1@,teixeira@ece.}osu.edu

***Abstract*—We report a rapid, robust full-wave methodology to model electromagnetic (EM) wave radiation by distributed current sources embedded in planar-layered media. Primitive causality-related numerical instabilities within the computation chain, induced by exponentially rising "distributed" current source spectrum functions, are addressed for both linear and aperture sources, leading to solution speed acceleration between one and two orders of magnitude versus space-domain superposition of Hertzian dipole fields. To overcome the instabilities, prior to numerical evaluation one analytically identifies and merges all exponentially rising and decaying terms, yielding an overall well-convergent and stable solution process. We present numerical results concerning sensors used to detect marine hydrocarbon reserves.**

Keywords*—*Electromagnetic analysis, stratified media.

I. Introduction

Sustained interest exists concerning EM fields in layered media [1]. Such geometries often (locally, near the sensor) well-approximates domains in exploration geophysics [2]–[20], for both onshore and offshore geophysical exploration modeling [21]–[28]. Planar-layered media, in particular, admits frequency and sensor-robust EM eigenfunction representations applicable for generally anisotropic and lossy media [28]. Said robustness property is particularly important in geophysical exploration problems, where measurements occur in diverse earth formations using complex multi-frequency sensor suites to aid geophysical parameter inversion [4], [29]. Inversion however is often computationally intensive, especially when forward engines are run many times to obtain a match between simulated and measured data; hence, accelerating the forward engine's solution speed remains a critical, ongoing effort.

For complex-shaped sensors, one could run the Hertzian current dipole field forward engine many times and then write said sensor's field via spatial superposition of the fields radiated from its equivalent Hertzian dipole constituents (i.e., evaluating the radiation integral in the space domain). The reason for exploring *spectral-domain* computation of the layered-medium radiation integral is due to solution speed, offering one or two orders of magnitude speed acceleration for 1-D or 2-D sources (resp.) [28] due to eliminating redundant source-*independent* calculations which consume the vast majority of computation time. The distributed source spectrum, which multiplicatively modifies the Hertzian dipole source-dependent amplitudes, contains exponentially rising terms however that must be analytically identified and merged with exponentially decaying terms to avoid numerically inaccurate or even undefined field results.

In Section II we outline the spectral-domain methodology ($\exp[-i\omega t]$ assumed); see [28] for further mathematical details. Section III contains numerical results. We provide some concluding remarks in Section IV.

II. Formulation

Consider a Hertzian dipole current source at $\mathbf{r}' = (x', y', z')$ within layer M. The homogeneous-medium "direct" field $\boldsymbol{\mathcal{E}}^d(\mathbf{r})$ has spectrum [28][1]

$$u(\Delta z)\sum_{n=1}^{2}\tilde{a}^d_{M,n}\tilde{\mathbf{e}}_{M,n}\mathrm{e}^{i\tilde{k}_{M,nz}\Delta z}+ u(-\Delta z)\sum_{n=3}^{4}\tilde{a}^d_{M,n}\tilde{\mathbf{e}}_{M,n}\mathrm{e}^{i\tilde{k}_{M,nz}\Delta z} \qquad \text{(II.1)}$$

and similarly for the scattered field's $\boldsymbol{\mathcal{E}}^s(\mathbf{r})$ spectrum. The distributed source's spectrum function multiplicatively modifies the $\{\tilde{a}^d_{M,n}\}$. For example, taking a L-meter long linear source (rect$[z]$ denotes rectangular window):

$$\boldsymbol{\mathcal{J}}(\mathbf{r}) = \cos\left(\frac{\pi z}{L}\right)\mathrm{rect}(z/L)\delta(x)\delta(y)\hat{\mathbf{z}} \qquad \text{(II.2)}$$

the spectral-domain amplitudes are now instead the $\{\tilde{a}^d_{M,n}\}$ multiplied by the source spectrum function $\tilde{\mathbf{J}}(\mathbf{k})$:

$$\frac{-\cos(\tilde{k}_{M,nz}L/2)}{L(\tilde{k}_{M,nz}-\pi/L)(\tilde{k}_{M,nz}+\pi/L)}\hat{\mathbf{z}} \qquad \text{(II.3)}$$

Analytically, the direct and scattered field spectrums are well-defined and lead to well-posed computation of $\boldsymbol{\mathcal{E}}^d(\mathbf{r})$ and $\boldsymbol{\mathcal{E}}^s(\mathbf{r})$ via 2-D Fourier integration [28]. However *practically* (i.e., numerically), observe that spectrum functions such as Eqn. (II.3) exponentially grow for complex-valued $\mathbf{k}$ (e.g., due to medium conductivity and/or integration path deformation).

[1] $\tilde{a}^d_{M,n}$ is the source-*dependent* amplitude of the nth mode in layer M, while $\tilde{\mathbf{e}}_{M,n}$ and $\tilde{k}_{M,nz}$ are the mode's source-*independent* eigenvector and eigenvalue, respectively. Here, $\Delta\mathbf{r} = \mathbf{r} - \mathbf{r}' = (\Delta x, \Delta y, \Delta z)$ and $u(z)$ is the Heaviside step function.

In a homogeneous medium, primitive causality considerations (i.e., cause before effect) dictate that the fields should decay with increasing source-observer separation along z. Mathematically, this has consequences on the (source and observation position-dependent) k_z-plane integration contours leading to numerically stable computations (and likewise for x vs. k_x, y vs. k_y). This is no problem for a single infinitesimal Hertzian dipole; however, for a distributed source, "receding" from one of its equivalent dipoles along z may correspond to "approaching" another one. Mathematically, this situation obfuscates proper k_z-plane contour choice and may lead to numerical instability (again, likewise for x vs. k_x, y vs. k_y). Using our linear antenna example to illustrate this point: When observing the field at $z = z_0$ ($-L/2 < z_0 < L/2$), equivalent Hertzian dipoles located below $z = z_0$ emit strictly up-going "direct" plane waves (and hence the k_z-plane real-axis path is equivalent to enclosing the upper-half k_z plane when computing this component of the direct field) while the equivalent Hertzian dipoles located above $z = z_0$ contribute strictly down-going "direct" plane waves (lower-half k_z plane equivalently enclosed). Hence even if observing at, say, $\mathbf{r} = (500, 0, z_0)$ [m], with the k_x contour deformation [28] imparting strong exponential decay, the linear source's spectrum function may itself exponentially grow (versus $|\text{Im}[k_z]|$) and lead to inaccurate or even overflown numerical field results. Identical conclusions apply to the scattered field, since it is excited by the direct field.

The remedy is to *analytically* (i) identify the distributed source spectrum function's ill-behaved component(s) and (ii) merge them with the standard Fourier kernel $\exp(ik_x\Delta x + ik_y\Delta y + ik_z\Delta z)$ arising in both single-dipole and distributed source field calculations, where for distributed sources $\mathbf{r}'$ is a suitably chosen "reference" location on the source distribution (e.g., the central point of a linear or rectangular current aperture). For the sources we consider [28], this means analytically merging the standard kernel's exponents with the exponent of each of the source spectrum's exponential function components. Considering said linear antenna example, calculating the nth plane wave mode's amplitude value now involves computing the well-behaved expression

$$-\frac{\tilde{a}^d_{M,n}}{2L(\tilde{k}_{M,nz} - \pi/L)(\tilde{k}_{M,nz} + \pi/L)} \times \left[e^{ik_x\Delta x + ik_y\Delta y + i\tilde{k}_{M,nz}(\Delta z + L/2)} + e^{ik_x\Delta x + ik_y\Delta y + i\tilde{k}_{M,nz}(\Delta z - L/2)} \right] \quad \text{(II.4)}$$

III. Results

We illustrate the proposed algorithm for enabling robust EM field computation in inhomogeneous and absorptive marine environments that typically constitute controlled-source EM (CSEM) deployment scenarios [21], [25], [26]. CSEM transmitters comprise very long wire antennas operating in the frequency range from about 0.01Hz to about 10Hz, for detection and characterization of thin hydrocarbon-bearing formations under the ocean floor. Such antennas exploit disturbances on the secondary field effected by the presence of such layers [27].

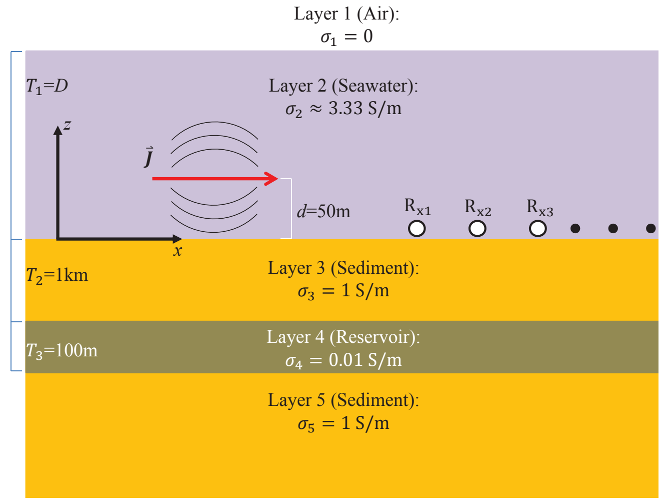

Fig. 1: Sensing geometry with hydrocarbon reservoir.

Consider the sensor geometry in Fig. 1, comprising one horizontal 100m-long linear antenna transmitter as well as multiple receivers (i.e., field observation points) located just above the seafloor (labeled R_{x1}, etc. in Fig. 1) in a D meter thick sea. The transmitter and any given receiver (separated by distance $x - x'$ along x from the transmitter) are all located within the xz plane ($y = 0$). To remove the relatively strong "direct" (homogeneous seawater) field component, which lacks influence from planar layering, we compute *scattered* fields (E^s_x, E^s_z) [28]. To moreover understand the *robustness*, of each observed field component's sensitivity (to the reservoir's presence), to air-sea interface EM reflections, during post-processing we compute magnitude ratios and phase differences of (E^s_x, E^s_z) for the geometries given by Fig. 1 (E^s_{x1}, E^s_{z1}) and an alternate (homogeneous sand seabed) geometry (E^s_{x2}, E^s_{z2}). The absolute value of the phase difference, as well as the magnitude ratio's deviation away from unity, are two potential indicators of reservoir sensitivity. We gain insight into the robustness of each measurement's sensitivity by examining the magnitude and phase swings for two different values of ocean depth D (100m and 500m).

Observe both the E^s_x (Figs. 2, 4) and E^s_z (Figs. 3, 5) measurements. For higher frequencies (≈1-10Hz), the 1km-thick upper sand layer attenuates reservoir-reflected fields and hence these fields lack significant reservoir sensitivity. Second, both the E^s_x and E^s_z measurements have reservoir sensitivity robust to air-sea reflections [28]. Interestingly, the E^s_x magnitude measurement shows *increased* reservoir sensitivity in shallower water. Third, the E^s_x and E^s_z measurements all show marked sensitivity for more remotely located receivers. The E^s_z measurements do show considerable sensitivity for more closely located receivers, but only for deeper oceans where

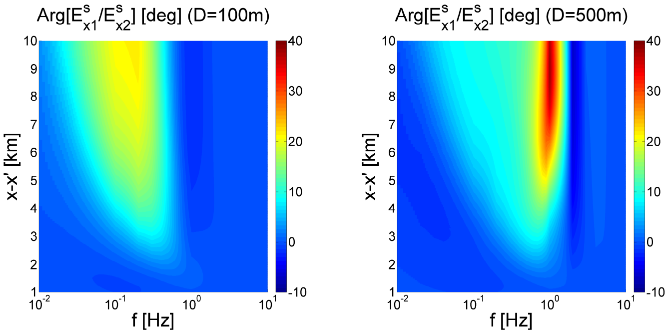

(a) (b)

Fig. 2: Phase shift ($\mathcal{E}_x^s$) between reservoir and reservoir-free scenarios.

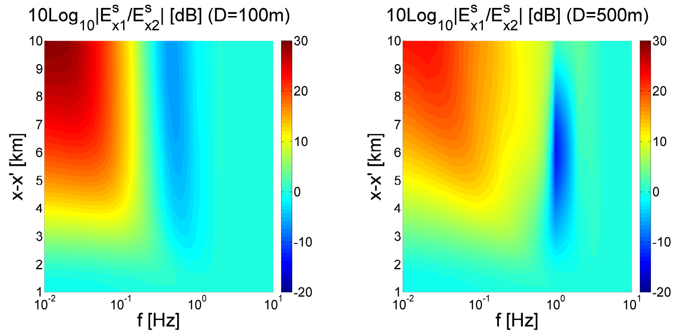

(a) (b)

Fig. 4: Magnitude ratio ($\mathcal{E}_x^s$) between reservoir and reservoir-free scenarios.

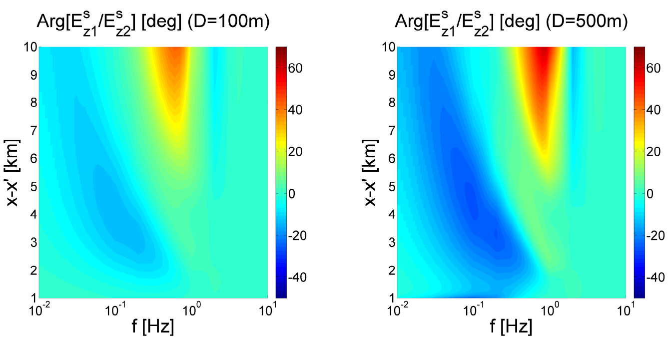

(a) (b)

Fig. 3: Same as Fig. 2, but $\mathcal{E}_z^s$.

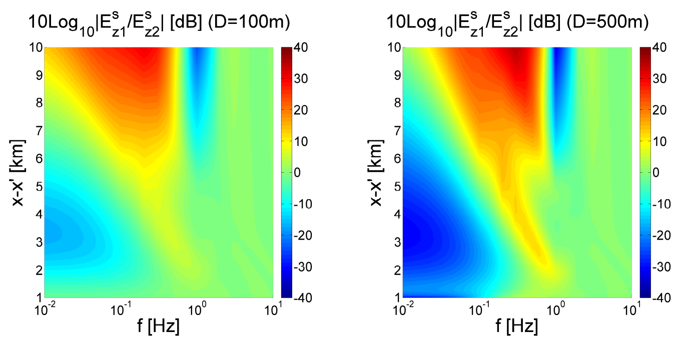

(a) (b)

Fig. 5: Same as Fig. 4, but $\mathcal{E}_z^s$.

the air-sea reflection is highly attenuated upon reaching the seafloor receivers.

IV. Conclusion

We discussed a full-wave spectral-domain method to robustly model EM radiation from distributed sources within planar-layered media. Distributed sources introduce exponentially rising spectrum functions inducing numerical instability. To remedy this, one analytically identifies and merges said functions with the standard, exponentially-decaying Fourier kernel, leading to a numerically stable algorithm featuring a one to two order of magnitude speed-up versus space-domain Hertzian dipole field superposition. Applying the algorithm to marine hydrocarbon remote sensing reveals the wealth of air-interface-robust reservoir information available from tensorial multi-frequency measurements.

Acknowledgment

NASA NSTRF and OSC support acknowledged.

References

[1] W. C. Chew, *Waves and Fields in Inhomogeneous Media*. Van Nostrand Reinhold, 1990.

[2] S. Davydycheva and T. Wang, "Modeling of Electromagnetic Logs in a Layered, Biaxially Anisotropic Medium," in *SEG Annual Meeting*. Tulsa, OK, USA: Society of Exploration Geophysicists, September 2011, pp. 494–498.

[3] B. Wei, T. Wang, and Y. Wang, "Computing the Response of Multi-Component Induction Logging in Layered Anisotropic Formation by the Recursive Matrix Method with Magnetic-Current-Source Dyadic Green's Function," *Chinese Journal of Geophysics*, vol. 52, no. 6, pp. 1350–1359, 2009.

[4] B. I. Anderson, T. D. Barber, and S. C. Gianzero, "The Effect of Crossbedding Anisotropy on Induction Tool Response," in *SPWLA 39th Annual Logging Symposium*. Houston, TX, USA: Society of Petrophysicists and Well-Log Analysts, May 1998, pp. 1–14.

[5] M. Zhdanov, W. Kennedy, and E. Peksen, "Foundations of Tensor Induction Well-Logging," *Petrophysics*, vol. 42, no. 6, pp. 588–610, November-December 2001.

[6] H. Wang, H. Tao, J. Yao, G. Chen, and S. Yang, "Study on the Response of a Multicomponent Induction Logging Tool in Deviated and Layered Anisotropic Formations by using Numerical Mode Matching Method," *Chinese Journal of Geophysics*, vol. 51, no. 5, pp. 1110–1120, 2008.

[7] Hongnian Wang, Honggen Tao, Jingjin Yao, and Ye Zhang, "Efficient and Reliable Simulation of Multicomponent Induction Logging Response in Horizontally Stratified Inhomogeneous TI Formations by

Numerical Mode Matching Method," *IEEE Transactions on Geoscience and Remote Sensing*, vol. 50, no. 9, 2012.

[8] J. Moran and S. Gianzero, "Effects of Formation Anisotropy on Resistivity-Logging Measurements," *Geophysics*, vol. 44, no. 7, pp. 1266–1286, 1979.

[9] D. Georgi, J. Schoen, and M. Rabinovich, "Biaxial Anisotropy: Its Occurrence and Measurement with Multicomponent Induction Tools," in *SPE Annual Technical Conference and Exhibition*. Houston, TX, USA: Society of Petroleum Engineers, September 2008, pp. 1–18.

[10] S. Liu and M. Sato, "Electromagnetic Well Logging Based on Borehole Radar," in *SPWLA 43rd Annual Logging Symposium*. Houston, TX, USA: Society of Petrophysicists and Well-Log Analysts, June 2002, pp. 1–14.

[11] M. Novo, L. Da Silva, and F. L. Teixeira, "Application of CFS-PML to Finite Volume Analysis of EM Well-Logging Tools in Multilayered Geophysical Formations," in *2006 12th Biennial IEEE Conference on Electromagnetic Field Computation*, 2006, pp. 201–201.

[12] Y.-K. Hue and F. L. Teixeira, "Analysis of Tilted-Coil Eccentric Borehole Antennas in Cylindrical Multilayered Formations for Well-logging Applications," *IEEE Transactions on Antennas and Propagation*, vol. 54, no. 4, pp. 1058–1064, April 2006.

[13] ——, "Numerical Mode-Matching Method for Tilted-Coil Antennas in Cylindrically Layered Anisotropic media with Multiple Horizontal Beds," *IEEE Transactions on Geoscience and Remote Sensing*, vol. 45, no. 8, pp. 2451–2462, Aug 2007.

[14] G.-S. Liu, F. Teixeira, and G.-J. Zhang, "Analysis of Directional Logging Tools in Anisotropic and Multieccentric Cylindrically-Layered Earth Formations," *IEEE Transactions on Antennas and Propagation*, vol. 60, no. 1, pp. 318–327, Jan 2012.

[15] H. G. Doll, "Introduction to Induction Logging and Application to Logging of Wells Drilled with Oil Base Mud," *Journal of Petroleum Technology*, vol. 1, no. 6, pp. 148–162, June 1949.

[16] K. Sainath, F. L. Teixeira, and B. Donderici, "Robust Computation of Dipole Electromagnetic Fields in Arbitrarily Anisotropic, Planar-Stratified Environments," *Phys. Rev. E*, vol. 89, p. 013312, Jan 2014.

[17] ——, "Complex-Plane Generalization of Scalar Levin Transforms: A Robust, Rapidly Convergent Method to Compute Potentials and Fields in Multi-Layered Media," *Journal of Computational Physics*, vol. 269, no. 0, pp. 403 – 422, 2014.

[18] K. Sainath and F. L. Teixeira, "Tensor Green's Function Evaluation in Arbitrarily Anisotropic, Layered Media using Complex-Plane Gauss-Laguerre Quadrature," *Phys. Rev. E*, vol. 89, p. 053303, May 2014.

[19] H. Moon, F. L. Teixeira, and B. Donderici, "Stable Pseudoanalytical Computation of Electromagnetic Fields from Arbitrarily-Oriented Dipoles in Cylindrically Stratified Media," *Journal of Computational Physics*, vol. 273, pp. 118 – 142, 2014.

[20] ——, "Computation of Potentials from Current Electrodes in Cylindrically Stratified Media: A Stable, Rescaled Semi-Analytical Formulation," *Journal of Computational Physics*, vol. 280, pp. 692 – 709, 2015.

[21] David Andreis and Lucy MacGregor, "Controlled-Source Electromagnetic Sounding in Shallow Water: Principles and Applications," *Geophysics*, vol. 73, no. 1, pp. F21–F32, 2008.

[22] Dylan Connell and Kerry Key, "A Numerical Comparison of Time and Frequency-Domain Marine Electromagnetic Methods for Hydrocarbon Exploration in Shallow Water," *Geophysical Prospecting*, vol. 61, no. 1, pp. 187–199, 2013.

[23] Chester Weiss, "The Fallacy of the Shallow-Water Problem in Marine CSEM Exploration," *Geophysics*, vol. 72, no. 6, pp. A93–A97, 2007.

[24] Peter Weidelt, "Guided Waves in Marine CSEM," *Geophysical Journal International*, vol. 171, no. 1, pp. 153–176, 2007.

[25] S. Ellingsrud, T. Eidesmo, S. Johansen, M. Sinha, L. MacGregor, and S. Constable, "Remote Sensing of Hydrocarbon Layers by Seabed Logging (sbl): Results from a Cruise Offshore Angola," *Leading Edge*, vol. 21, no. 10, pp. 972–982, October 2002.

[26] T. Eidsmo, S. Ellingsrud, L. MacGregor, S. Constable, M. Sinha, S. Johansen, F. Kong, , and H. Westerdahl, "Sea Bed Logging (SBL), A New Method for Remote and Direct Identification of Hydrocarbon Filled Layers in Deepwater Areas," *First Break*, vol. 20, no. 3, pp. 144–152, March 2002.

[27] E. Um and D. Alumbaugh, "On the Physics of the Marine Controlled-Source Electromagnetic Method," *Geophysics*, vol. 72, no. 2, pp. WA13–WA26, 2007.

[28] K. Sainath and F. L. Teixeira, "Spectral-Domain-Based Scattering Analysis of Fields Radiated by Distributed Sources in Planar-Stratified Environments with Arbitrarily Anisotropic Layers," *Phys. Rev. E*, vol. 90, p. 063302, Dec 2014.

[29] Y.-H. Chen, D. Omeragic, V. Druskin, C.-H. Kuo, T. Habashy, A. Abubakar, and L. Knizhnerman, "2.5D FD Modeling of EM Directional Propagation Tools in High-Angle and Horizontal Wells," in *SEG Annual Meeting*. Tulsa, OK, USA: Society of Exploration Geophysicists, 2011, pp. 422–426.